Deterministic Chaos in the Dynamics of a Freely Jointed Chain with Three Degrees of Freedom

Georg R. Siegert, Roland G. Winkler, and Peter Reineker
Abteilung Theoretische Physik, Universität Ulm, 7900 Ulm, Germany

Z. Naturforsch. **48a**, 584–594 (1993); received February 1, 1993

The dynamics of a short freely jointed chain of three segments is investigated numerically. The chain consists of mass points connected by massless rigid rods, its initial and final points being fixed. Thus the chain represents a holonomically constrained system with three degrees of freedom. It is shown that the motion of the mass points can be chaotic; the occurrence of chaos depends on the initial conditions of the motion, the end-to-end distance of the chain, and the angular momentum about the axis of the stretching direction. Moreover, the chain more likely exhibits regular than chaotic behavior. The numerical results are presented in the form of Poincaré surfaces of section, including the use of a slice technique, as well as in the form of power spectra.

Key words: Deterministic chaos; Freely jointed chain; Constraints; Poincaré surface of section; Powerspectra.

1. Introduction

The occurrence of chaos in systems with two and three degrees of freedom has been demonstrated in many cases [1–4]. Usually systems are studied, where the necessary nonlinearities are introduced via potentials or boundary conditions [1–5]. Much less is known about chaos in autonomous systems with constraints.

While working with models for polymeric chains we investigated also in detail the dynamics of nonlinearly constraint systems with two and three degrees of freedom [6–8]. In this paper we present the results of the investigations for the latter systems with stress on the chaotic behavior. Investigations for longer chains are devoted mainly to polymeric properties, such as stress-strain relations, and are published in a separate paper [26].

Polymeric chains are often (microscopically) modelled as freely jointed chains. This model has been successfully applied to calculations of the entropy, elastic properties and other quantities of single chains by analytically evaluating the partition function [9–16]. However, the model is not only used in analytical theoretical investigations but also in a slightly modified form in computer simulations. Instead of simply describing the chain in terms of segments, the dynamical treatment requires the modelling of chains as an ensemble of mass points which are connected in some way. There are in principle two different classical models: the flexible and the rigid chain model. In the flexible chain model the mass points are connected by harmonic or anharmonic springs [17, 18]. In the limit of an infinite spring constant these chains provide the results of the analytical statistical treatment of the freely jointed chain [17, 19]. In the rigid chain model the mass points are connected by massless rigid rods [6, 7, 20–23]. Due to these constraints, there is a coupling between the configurations of the chain and its kinetic energy. Thus, the equilibrium distribution in phase space is different for the two models [7, 24].

In computer simulations it is important to achieve the correct thermalization of all degrees of freedom. This is certainly fulfilled if the system is globally chaotic. In a previous paper we showed that a short two dimensional chain consisting of mass points connected by rigid segments exhibits chaotic motion [6, 7, 22, 23]. The purpose of this paper is to investigate the dynamical behavior of a short chain in three dimensions. Our model chain (see Fig. 1) consists of two mass points mobile in three dimensions. The points are connected by massless rigid rods, and the initial and final points of the first and fourth rod, respectively are fixed. Taking into account the constraints, the system has three degrees of freedom and two globally conserved quantities: the energy and the angular momentum about the stretching axis. The nonlinearities, necessary for the existence of chaotic behavior, are introduced by the constraints; no potential is

Reprint requests to Prof. Dr. P. Reineker, Abteilung Theoretische Physik, Universität Ulm, Albert-Einstein-Allee 11, D-W-7900 Ulm, FRG.

0932-0784 / 93 / 0400-0584 $ 01.30/0. – Please order a reprint rather than making your own copy.

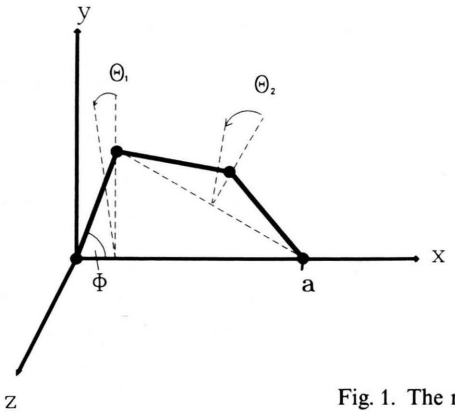

Fig. 1. The model chain.

taken into account. The occurrence of chaos in systems with three degrees of freedom has up to now only rarely been studied. In the paper we use two different techniques of analyzing the dynamics: the method of Poincaré surfaces of section combined with a slice technique and power spectra [1–3, 25]. To our knowledge, a system with three degrees of freedom and nonlinearities introduced by constraints has not been studied before.

The paper is organized as follows: In Sect. 2 the equations of motion are derived. Section 3 presents and discusses the numerical results. Finally, Sect. 4 summarizes our findings.

2. Equations of Motion

We consider a polymeric chain consisting of four mass points which are connected by massless rigid rods of length l (see Figure 1). One of the end points is fixed at the origin of a cartesian coordinate system, the other one at a point a on the x-axis. The remaining two points have to satisfy the constraints

$$\boldsymbol{r}_1^2 - l^2 = 0\,, \tag{1}$$

$$(\boldsymbol{r}_2 - \boldsymbol{r}_1)^2 - l^2 = 0\,, \tag{2}$$

$$(\boldsymbol{a} - \boldsymbol{r}_2)^2 - l^2 = 0\,, \tag{3}$$

where $\boldsymbol{a} = a\,\boldsymbol{e}_x$. Since there is no potential energy, the Lagrangian reads

$$L = \tfrac{1}{2}\sum_{i=1}^{2} m\,\dot{\boldsymbol{r}}_i^2 + \tfrac{1}{2}\sum_{i=1}^{3} \tilde{\lambda}_i((\boldsymbol{r}_{i+1} - \boldsymbol{r}_i)^2 - l^2)\,. \tag{4}$$

In this Lagrangian we have assumed that the masses of the two points are equal, and the constraints have been taken into account via Lagrangian multipliers $\tilde{\lambda}_i$. Also, we used the convention $\boldsymbol{r}_1 = 0$, $\boldsymbol{r}_3 = \boldsymbol{a}$. The equations of motion read [7, 8, 26]

$$m\ddot{\boldsymbol{r}}_1 = \tilde{\lambda}_1 \boldsymbol{r}_1 + \tilde{\lambda}_2(\boldsymbol{r}_1 - \boldsymbol{r}_2)\,, \tag{5}$$

$$m\ddot{\boldsymbol{r}}_2 = \tilde{\lambda}_2(\boldsymbol{r}_2 - \boldsymbol{r}_1) + \tilde{\lambda}_3(\boldsymbol{r}_2 - \boldsymbol{a}) \tag{6}$$

and contain only forces of constraint on the right hand side. It is useful to introduce dimensionless variables

$$\boldsymbol{r}_i(t) = l\,\boldsymbol{\varrho}_i(\tau), \quad \boldsymbol{a} = l\,\boldsymbol{\alpha}\,, \tag{7}$$

$$t = \sqrt{\frac{m\,l^2}{E}}\,\tau\,, \tag{8}$$

$$\tilde{\lambda}_i(t) = \frac{E}{l^2}\,\lambda_i(\tau)\,, \tag{9}$$

$$\dot{\boldsymbol{r}}_i(t) = \sqrt{\frac{E}{m}}\,\dot{\boldsymbol{\varrho}}_i(\tau)\,, \tag{10}$$

$$\ddot{\boldsymbol{r}}_i(t) = \frac{E}{m\,l}\,\ddot{\boldsymbol{\varrho}}_i(\tau)\,, \tag{11}$$

where E is the total energy.

Thus the problem is reduced to solving the set of differential equations

$$\ddot{\boldsymbol{\varrho}}_1 = \lambda_1\,\boldsymbol{\varrho}_1 + \lambda_2(\boldsymbol{\varrho}_1 - \boldsymbol{\varrho}_2)\,, \tag{12}$$

$$\ddot{\boldsymbol{\varrho}}_2 = \lambda_2(\boldsymbol{\varrho}_2 - \boldsymbol{\varrho}_1) + \lambda_3(\boldsymbol{\varrho}_2 - \boldsymbol{\alpha})\,, \tag{13}$$

where $\dot{\boldsymbol{\varrho}} = \dfrac{\mathrm{d}}{\mathrm{d}\tau}\,\varrho$. Owing to the three constraints, the system has three degrees of freedom. Since we have a Hamiltonian system, the total energy is conserved. Additionally, due to the rotational symmetry about the x-axis, the x-component of the angular momentum

$$L_x = \varrho_{1y}\,\dot{\varrho}_{1z} - \varrho_{1z}\,\dot{\varrho}_{1y} + \varrho_{2y}\,\dot{\varrho}_{2z} - \varrho_{2z}\,\dot{\varrho}_{2y} \tag{14}$$

is also conserved. These two integrals of motion confine the trajectory of the system to a four dimensional subspace of the six dimensional phase space. In the equations of motion we have the three parameters E, α, and L_x. From (8) it is obvious that E can be incorporated in the time scaling. Therefore, in the following we will discuss the influence of the extension α and of the angular momentum L_x on the dynamics of the system.

To integrate the equations of motion (12), (13), it is necessary to eliminate the Lagrangian multipliers by expressing them in terms of $\{\boldsymbol{\varrho}_i\}$ and $\{\dot{\boldsymbol{\varrho}}_i\}$. This is accomplished by differentiating the constraints and sub-

sequently introducing them into the equations of motion. The result for the multipliers reads

$$\lambda_1 = \frac{1}{N}\left[(\dot{\varrho}_2 - \dot{\varrho}_1)^2 C + \dot{\varrho}_1^2 (2 - B^2) + \dot{\varrho}_2^2 CB\right], \quad (15)$$

$$\lambda_2 = \frac{1}{N}\left[(\dot{\varrho}_2 - \dot{\varrho}_1)^2 + \dot{\varrho}_1^2 C + \dot{\varrho}_2^2 B\right], \quad (16)$$

$$\lambda_3 = \frac{1}{N}\left[(\dot{\varrho}_2 - \dot{\varrho}_1)^2 B + \dot{\varrho}_1^2 CB + \dot{\varrho}_2^2 (2 - C^2)\right] \quad (17)$$

with

$$B = (\varrho_2 - \varrho_1)(\alpha - \varrho_2), \quad (18)$$

$$C = \varrho_1 \varrho_2 - 1, \quad (19)$$

$$N = B^2 + C^2 - 2. \quad (20)$$

The fact that the multipliers are highly nonlinear functions of the coordinates and velocities lets us expect that deterministic chaos may occur in the dynamics of the chain. If the velocities $\{\dot{\varrho}_i\}$ are taken as independent variables, one eventually obtains a system of 12 nonlinear, first order differential equations. These were integrated numerically using a fourth order Adams-Bashforth-Moulton predictor-corrector method [27]. The method proved to be very stable and suitable for the solution of the equations of motion including constraints. The conserved quantities (E, L_x) were constant within 0.01–0.1% of the desired value.

We wish to stress once more that there are only four truly independent variables: three coordinates (owing to the three constraints) and one velocity (owing to the three time derivatives of the constraints and the two integrals of motion). These four variables may be chosen at convenience. In the following section we represent numerical solutions of the equations of motion in form of Poincaré surfaces of section and power spectra for various values of α and L_x. We do not discuss Liapunov exponents [1] here, since we found unexpected results, which allow no clear distinction even between regular and chaotic trajectories in a 2-dimensional constraint system of four segments [6]. We further investigate this effect and discuss it in a future paper.

3. Numerical Results

3.1. Poincaré Surface of Section

The dynamical behavior of Hamiltonian systems with more than one degree of freedom is often analysed with the help of Poincaré surfaces of section [1, 2, 6–8]. Since our system is confined to a four dimensional manifold (hyper-surface) in the six dimensional phase space, the Poincaré surface of section Σ represents a three dimensional manifold, i.e. the intersections of a trajectory with the Poincaré surface of section could fill a three dimensional hyper-surface [8]. Because a three dimensional surface can not be presented graphically, we additionally used the slice technique introduced by Hénon [25]. However, it should be remarked that this technique has a disadvantage: the points should be evenly spread over the four dimensional hyper-surface, and a fairly high density in phase space is necessary to obtain satisfactory results. This often requires very long integration intervals.

As just mentioned, due to the conserved quantities E and L_x and the introduction of a surface of section, we will obtain phase points which lie on a three dimensional manifold. If a third integral of motion exists, we will find the intersections of the trajectory with the surface of section distributed over a two dimensional manifold. However, a system with three degrees of freedom and three integrals of motion is integrable. Therefore, in the system considered here, the integrable case is represented by the distribution of the intersection points of the trajectory with the surface of section over a two dimensional surface. A further integral of motion (over-integrable case) leads to a concentration of the intersection points on curves.

A special feature of dynamic systems with more than two degrees of freedom is the occurrence of Arnold-diffusion. This means that chaotic trajectories are no longer trapped between regular tori, as in the case of a system with two degrees of freedom, but can reach any point in the available phase space, i.e. they can wander over the so-called Arnold-web [1]. Therefore, in one diagram we can only plot one trajectory. Thus it is difficult to show a large number of trajectories and a concise overview of the dynamics can not be given. For lack of space, the following maps and spectra only show the results for a small fraction of the studied trajectories and are supposed to exemplify certain salient features of the system [8].

In our case, the surface of section was defined by the condition $z_1 = 0$, meaning that all mappings show states of the system where the first mass point was in the xy-plane. Two coordinates and one velocity remained to be chosen. We arbitrarily selected x_1, z_2, and $\dot{z}_1$.

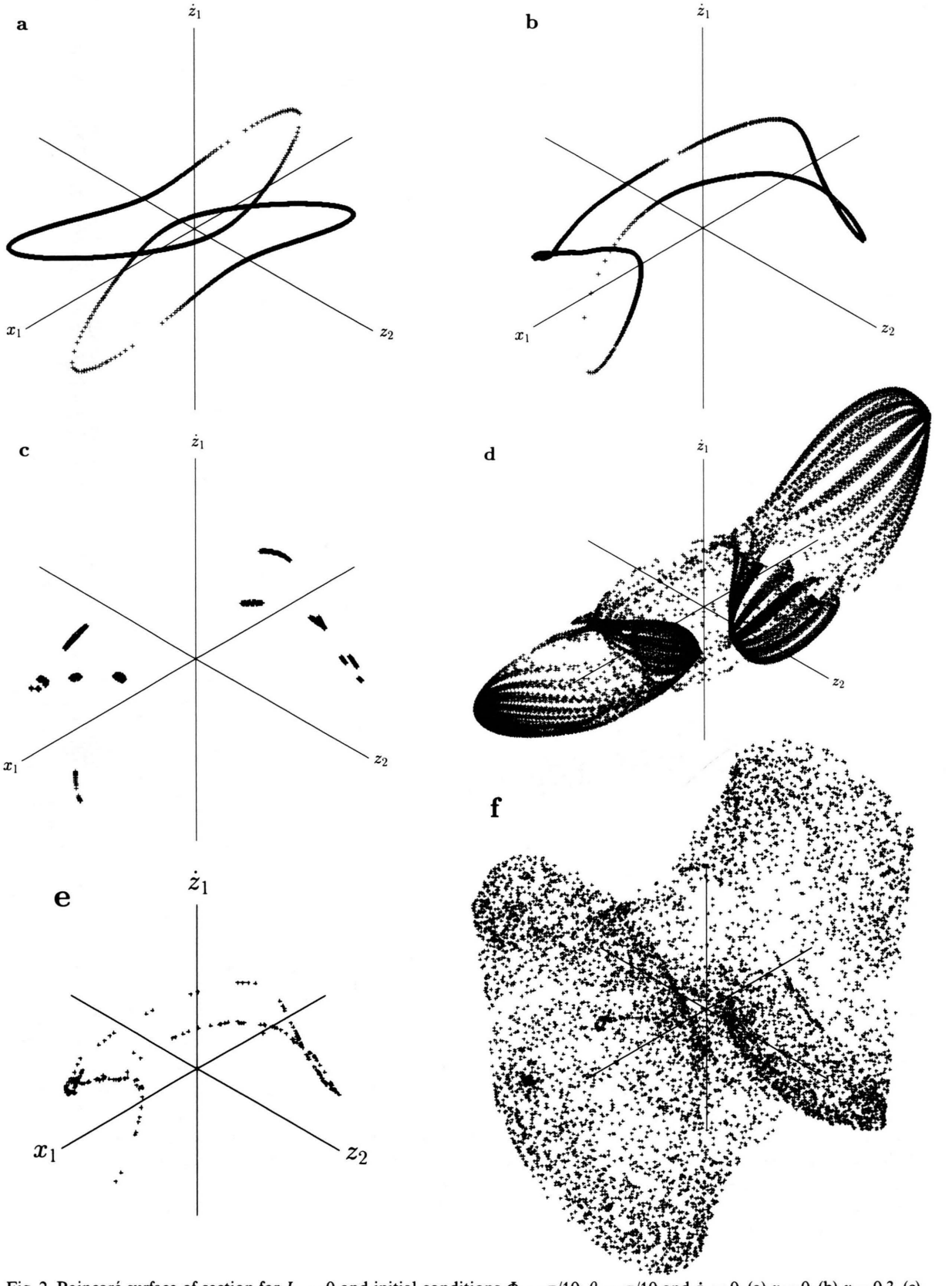

Fig. 2. Poincaré surface of section for $L_x = 0$ and initial conditions $\Phi_1 = \pi/10$, $\theta_2 = \pi/10$ and $\dot{z}_1 = 0$. (a) $\alpha = 0$. (b) $\alpha = 0.3$. (c) $\alpha = 0.34$. (d) $\alpha = 0.36$. (e) The first 220 points for $\alpha = 0.361$. (f) The parameter α is the same as in (e), except that now all points are shown. This is a good example of Arnold-diffusion.

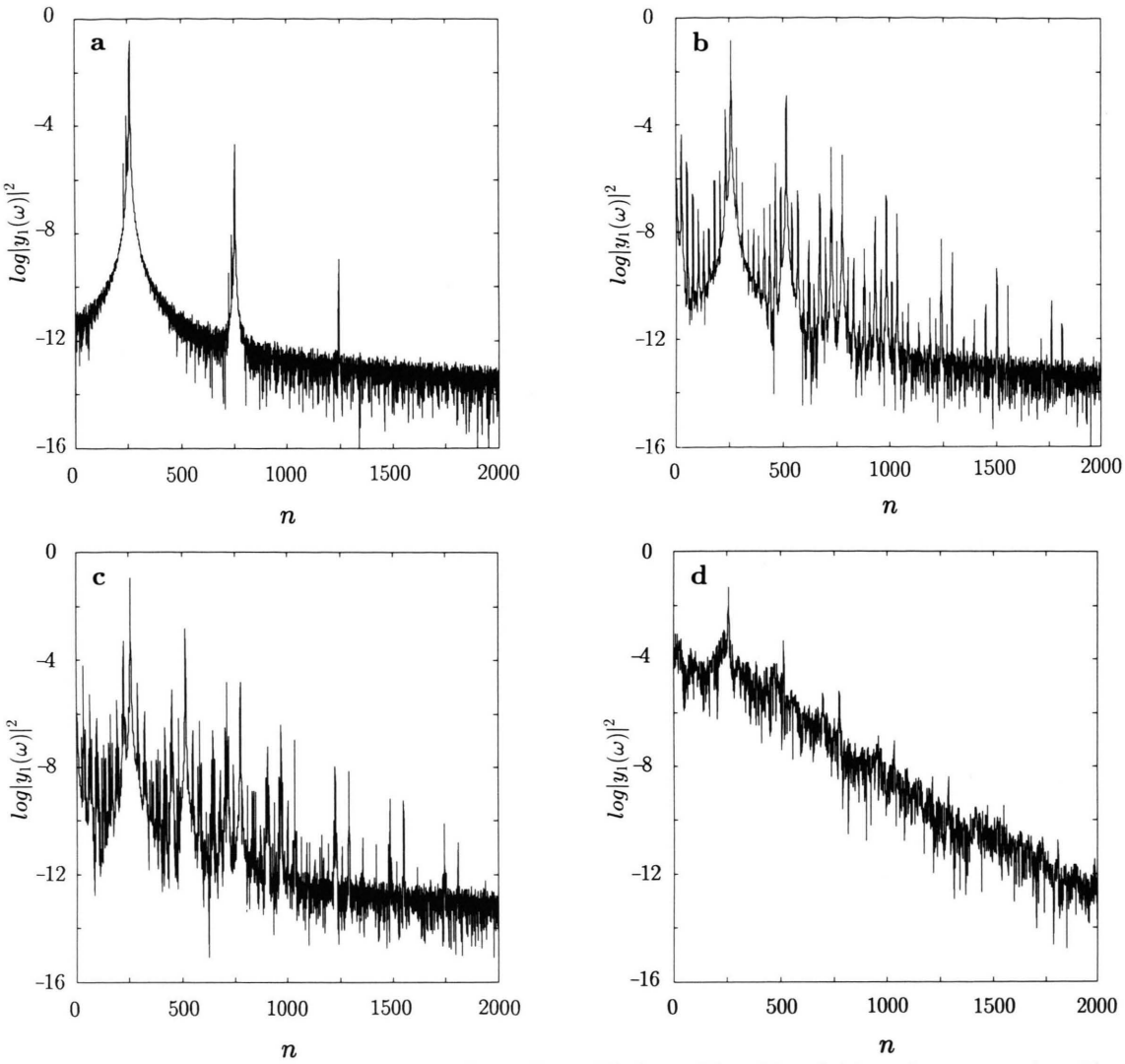

Fig. 3. Power spectra for $L_x = 0$ and initial conditions $\Phi_1 = \pi/10$, $\theta_2 = \pi/10$ and $\dot{z}_1 = 0$. (a) $\alpha = 0$; corresponds to Figure 2a. (b) $\alpha = 0.3$; corresponds to Figure 2b. (c) $\alpha = 0.34$; corresponds to Figure 2c. (d) $\alpha = 0.361$; corresponds to Figs. 2e and 2f.

3.2. Power Spectra

The main characteristic of regular trajectories is that their motion is determined by f fundamental frequencies (f being the number of degrees of freedom). In contrast, the irregular nature of chaotic motion implies the occurrence of a continuous frequency spectrum [3]. The spectrum of a regular trajectory should therefore be characterized by a few sharp peaks (fundamental frequencies and harmonics), whereas a chaotic trajectory should produce a continuous signal.

The spectra in Figs. 3, 5, and 8 show the square of the modulus of the Fourier-transform of the y-component of the first mass point ($|y_1(\omega)|^2$). A Fast-Fourier-Transform algorithm was employed, which implies that the number of sampled points was always equal to a power of two. Samples were taken every $\Delta\tau = 5 \times 10^{-2}$. In all spectra with the exception of Fig. 5b, $N = 2^{15}$ samples were taken, leading to a transform interval of duration $T = 1638.4$. In Fig. 5b 2^{18} samples were taken corresponding to $T = 13\,107.2$. The frequencies on the abscissa are distinguished by n, which

is defined by

$$\omega_n = n\frac{2\pi}{T} = n\frac{2\pi}{N\Delta\tau}. \tag{21}$$

The modulus of the Fourier-Transform is presented in a logarithmic scale.

3.3. *Influence of* α

Figures 2a through 2f were all obtained with the initial conditions

$$\Phi_1 = \frac{\pi}{10}, \tag{22}$$

$$\theta_2 = \frac{\pi}{10}, \tag{23}$$

$$\dot{z}_1 = 0. \tag{24}$$

Φ_1 is the angle between the first chain-segment and the x-axis, θ_2 the angle by which the second masspoint is rotated out of the xy-plane (cf. Figure 1). The x-component of the angular momentum L_x was set equal to 0.

Figure 2a shows the Poincaré surface of section for $\alpha = 0$. In this case one expects to find a regular trajectory, because not only L_x but also the total angular momentum is conserved, and therefore the system is integrable. In fact, it is over-integrable as can be seen by the fact that the intersections of the trajectory with the surface of section do not cover a two dimensional surface but rather are positioned along curves. The two curves exhibit parity invariance, which is a reflection of the fact that the system is parity symmetric for $\alpha = 0$.

The spectrum of Fig. 3a has three fundamental frequencies (ν_1, ν_2, ν_3), and the harmonics can all be calculated using

$$\nu_i = |a_1^{(i)}\nu_1 + a_2^{(i)}\nu_2 + a_3^{(i)}\nu_3|,$$

where the $a_j^{(i)}$'s ($j = 1, 2, 3$) are integers. It is interesting to note that all harmonics are of odd order, i.e. the sum over a_j is always an odd number.

Stretching the chain to a length of $\alpha = 0.3$ (Fig. 2b) destroys the parity invariance (as expected), but the motion remains over-integrable. In the spectrum shown in Fig. 3b this increase in α leads to an increase in the number of frequency peaks (which means that the motion becomes more complicated). Furthermore, now even order peaks also appear.

An interesting effect can be observed in the case $\alpha = 0.34$ (Fig. 2c): the curve dissolves into a chain of small islands in the vicinity of the original curve. These islands again form closed curves, which means that the system still behaves in an over-integrable manner. The corresponding spectrum of Fig. 3c gives no indication of this effect because it does not look very different from that of Figure 3b. It should be mentioned that this island structure was only observed for this value of α ($\alpha = 0.34$). In a system with two degrees of freedom, island structures appear in the transition region between regular and chaotic motion [1, 2]. However, our system of three degrees of freedom still displays regular motion for values of α up to 0.36. In all these cases the Poincaré surfaces of section show curves. For the initial condition (22)–(24) we never found a trajectory where the points were evenly spread over a two dimensional surface corresponding to regular motion.

The result for $\alpha = 0.36$ is shown in Figure 2d. The points lie on "bands". It was impossible to judge whether the points are spread on a surface or not, because they practically all accumulate in the vicinity of $x = 1$ or $x = -1$. The corresponding spectrum, which is not shown here, looks just like Figure 3c. The power spectra therefore give no indication of the dramatic differences which are observed in the Poincaré surfaces of section.

The transition into chaos occurs at $\alpha = 0.361$. Figure 2e displays the first 220 points in the time evolution. They appear to be distributed on a curve resembling those obtained for smaller values of α (e.g. $\alpha = 0.3$). The following points (Fig. 2f) begin to fill the entire accessible region of the space of section. This is an example of Arnold-diffusion: at first the system is trapped close to a stable torus only to "break free" at a certain point in time and then wander all over the Arnold-web. The corresponding spectrum (Fig. 3d) is decidedly chaotic: an unstructured and noisy signal with exponentially decreasing amplitude.

The trajectories remain chaotic for values of α between 0.361 and 1.8. At $\alpha = 1.8$ another transition occurs, this time back towards regular motion. For $1.8 < \alpha < 3$ the motion remains regular and the surfaces of section show that the system is again over-integrable. The spectra indicate that the dominating fundamental frequency is shifted towards higher values of n, which is understandable when considering that a large value of α forces the mass points closer to the x-axis which, at constant energy, causes higher frequencies.

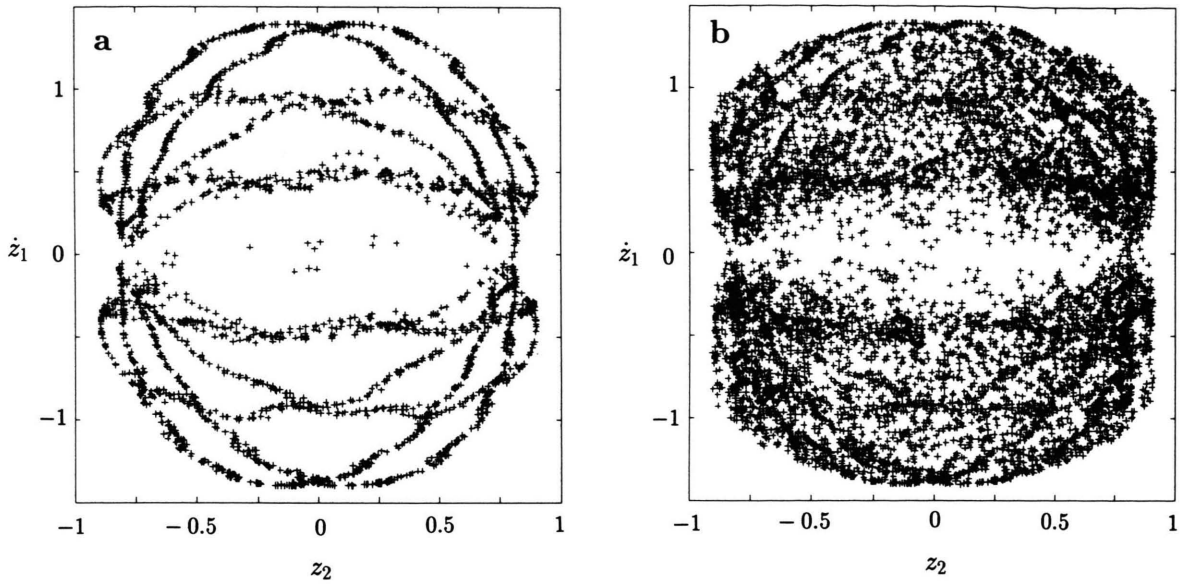

Fig. 4. Another example of Arnold-diffusion. The Poincaré surface of section for $\alpha = 0.165$, $L_x = 0$ and initial conditions $\Phi_1 = \pi/4$, $\theta_2 = \pi/4$ and $\dot{z}_1 = 0.4$ is shown. The points are projected into the $(z_2, \dot{z}_1)$-plane. (a) The first 2700 points. (b) All 8076 points.

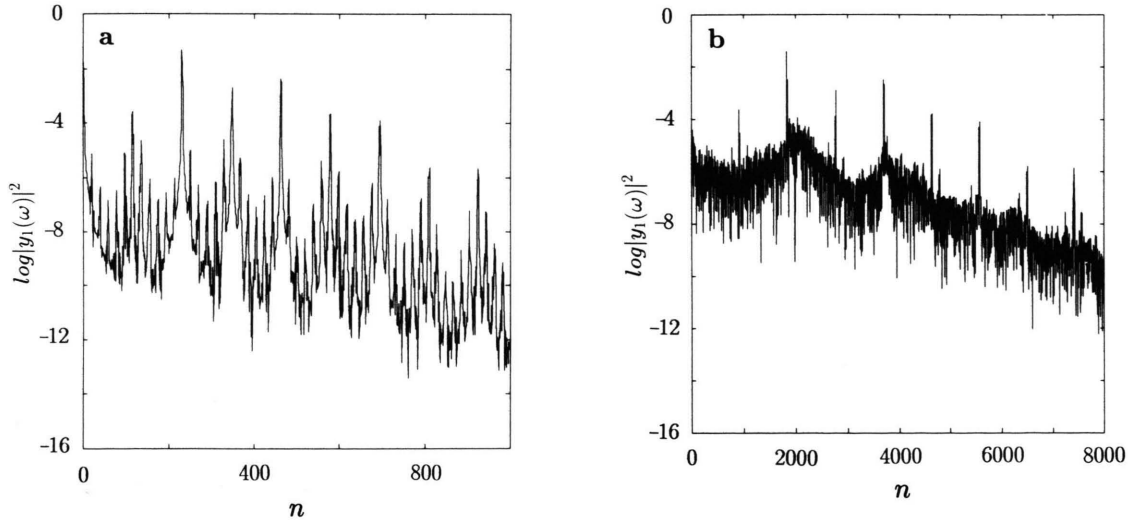

Fig. 5. Power spectra for $\alpha = 0.165$, $L_x = 0$ and initial conditions $\Phi_1 = \pi/4$, $\theta_2 = \pi/4$ and $\dot{z}_1 = 0.4$. (a) Result for the transform of 2^{15} points, i.e. over an interval $\tau = 1638.4$. (b) Result for the transform of 2^{18} points, i.e. over an interval $\tau = 13\,107.2$.

The question is: is this behavior of the system still valid when varying the initial condition? Results for different initial conditions (with L_x remaining equal to 0) indicate that indeed it is: the motion is regular (and mostly over-integrable) for small values of α and for $\alpha > 1.9$, there being a mainly chaotic region inbetween.

Figures 4a and 4b show another example of Arnold-diffusion. The initial conditions were: $\Phi_1 = \pi/4$, $\theta_2 = \pi/4$ and $\dot{z}_1 = 0.4$. The angular momentum L_x was again equal to 0. The system stays trapped (Fig. 4a) for a fairly long period of time ($\tau = 10\,000$). This example illuminates one of the problems encountered while

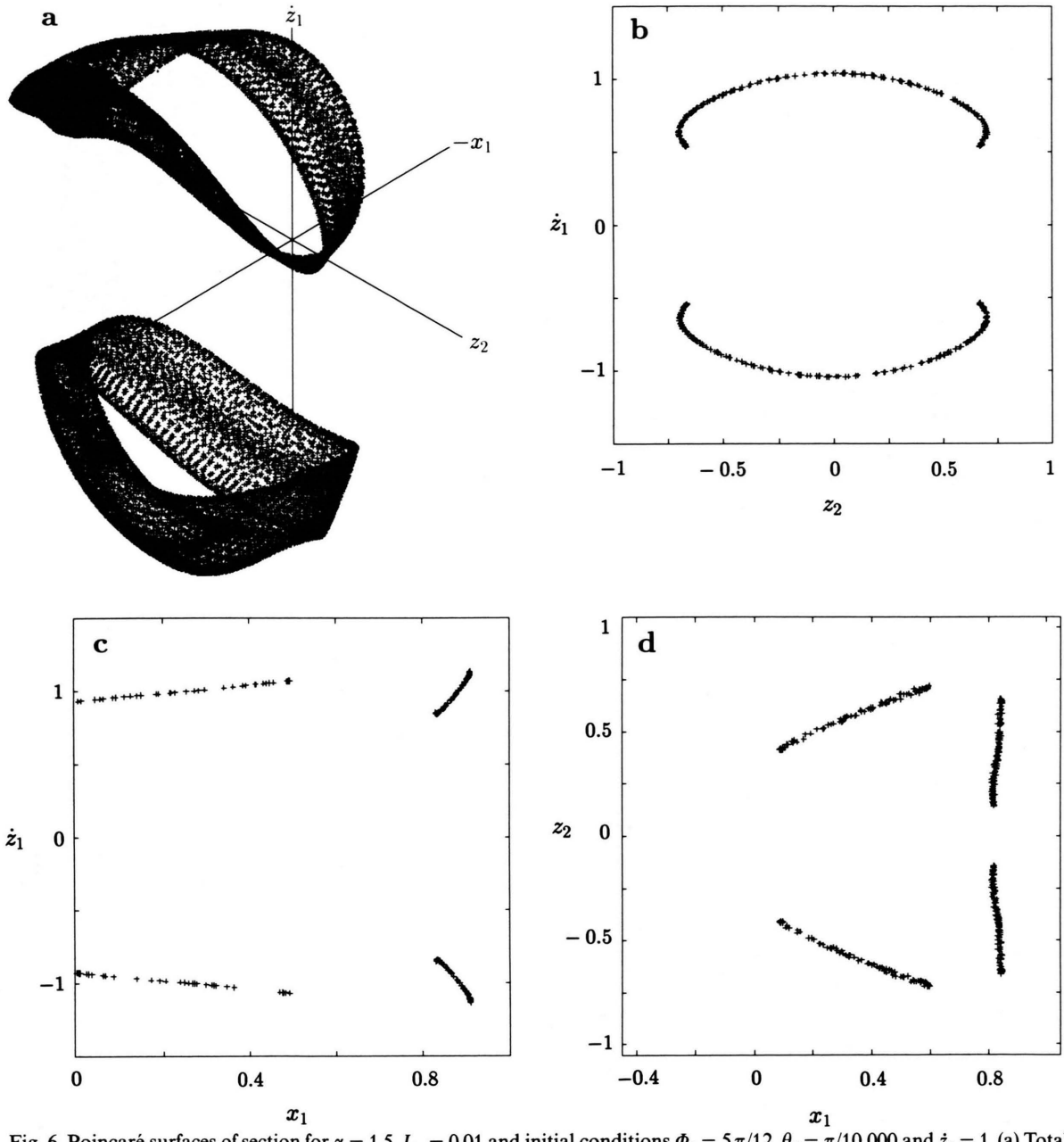

Fig. 6. Poincaré surfaces of section for $\alpha = 1.5$, $L_x = 0.01$ and initial conditions $\Phi_1 = 5\pi/12$, $\theta_2 = \pi/10\,000$ and $\dot{z}_1 = 1$. (a) Total view of all points. (b) Slice of thickness $\Delta x_1 = 0.01$ parallel to the $(z_2, \dot{z}_1)$-plane, centered at $x_1 = 0.4$. (c) Slice of thickness $\Delta z_2 = 0.01$ parallel to the $(x_1, \dot{z}_1)$-plane, centered at $z_2 = 0$. (d) Slice of thickness $\Delta \dot{z}_1 = 0.01$ parallel to the (x_1, z_2)-plane, centered at $\dot{z}_1 = 0.8$.

working with the Fourier-spectrum technique: the spectrum with 2^{15} sample points (Fig. 5a) does not necessarily indicate chaotic behavior. This is due to the fact that in this case the total interval of integration was only $T = 1638.4$. Only after sampling 2^{18} points does the chaotic nature become evident (Figure 5b). The visible onset of chaos is not an artifact of the numerical integration algorithm because the conserved quantities agree with the given values within 0.1%. However, it sensitively depends on the time

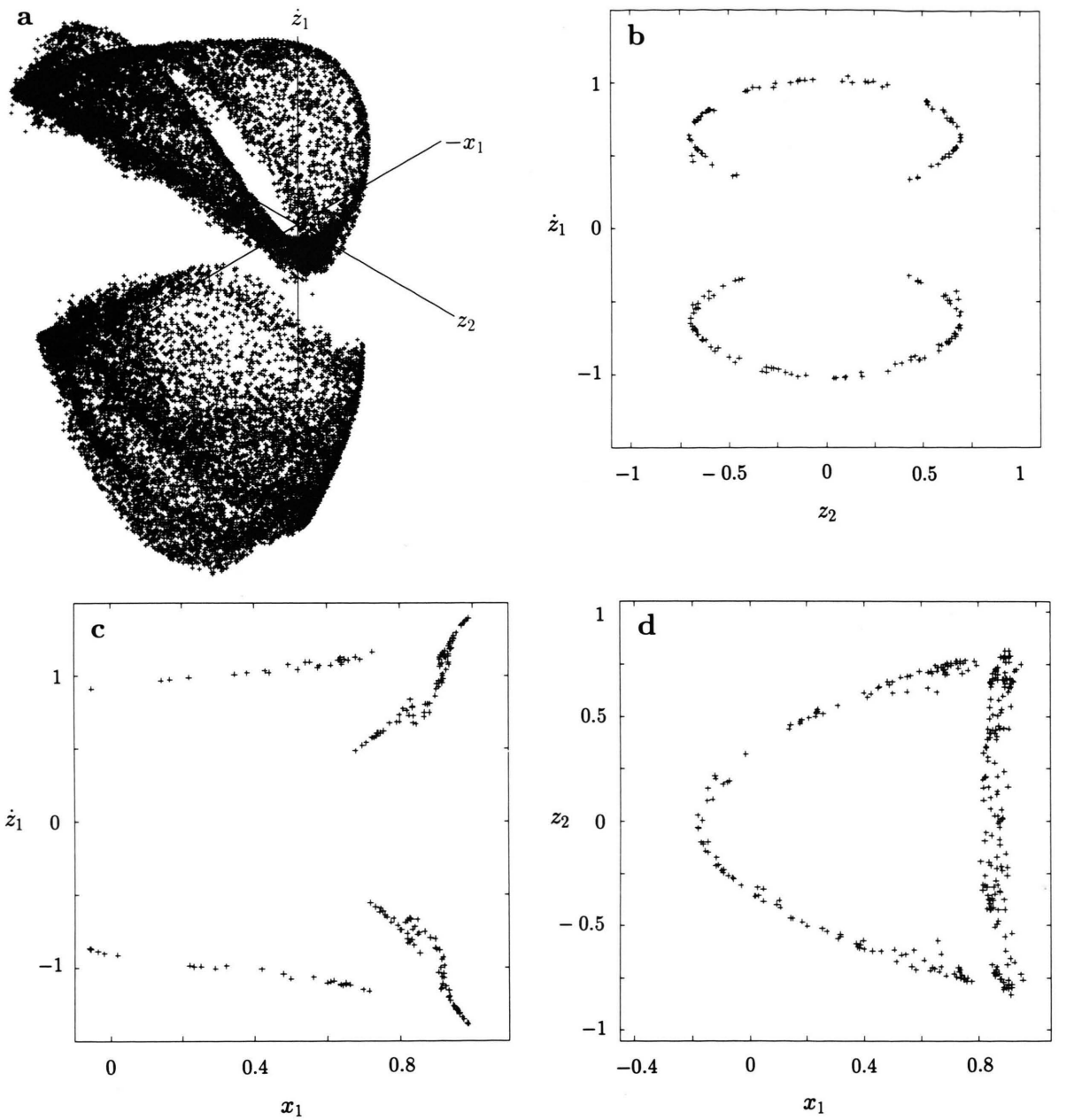

Fig. 7. Poincaré surfaces of section for $\alpha = 1.5$, $L_x = 0.02$ and initial conditions $\Phi_1 = 5\pi/12$, $\theta_2 = \pi/10\,000$ and $\dot{z}_1 = 1$. (a) Total view of all points. (b) Slice of thickness $\Delta x_1 = 0.01$ parallel to the $(z_2, \dot{z}_1)$-plane, centered at $x_1 = 0.4$. (c) Slice of thickness $\Delta z_2 = 0.01$ parallel to the $(x_1, \dot{z}_1)$-plane, centered at $x_2 = 0$. (d) Slice of thickness $\Delta \dot{z}_1 = 0.01$ parallel to the (x_1, z_2)-plane, centered at $\dot{z}_1 = 0.8$

step. For a smaller time step the chaos will be evident after a longer integration interval. Thus, one has to be careful when interpreting spectra of trajectories that are in an area of transition between chaotic and regular motion.

3.4. Influence of L_x

The trajectory (not shown here) for $\alpha = 1.5$, $\Phi_1 = 5\pi/12$, $\theta_2 = \pi/10\,000$, $\dot{z}_1 = 1$ and $L_x = 0$ is regular and over-integrable [8]. Already a slight increase of L_x to

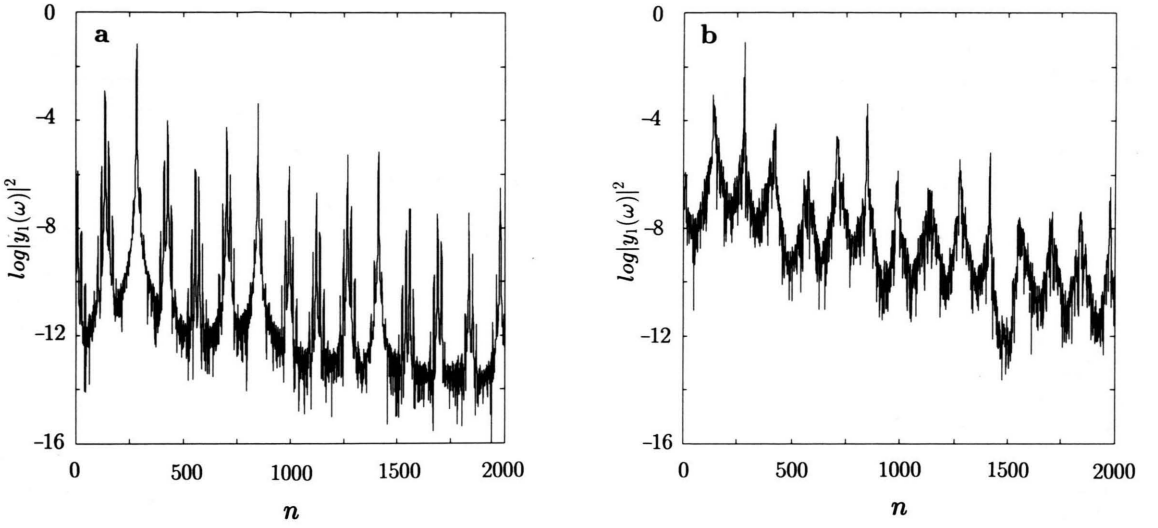

Fig. 8. (a) Power spectrum for $\alpha = 1.5$, $L_x = 0.01$ and initial conditions $\Phi_1 = 5\pi/12$, $\theta_2 = \pi/10\,000$ and $\dot{z}_1 = 1$. It corresponds to the sections in Figure 6. (b) Power spectrum for $\alpha = 1.5$, $L_x = 0.02$ and initial conditions $\Phi_1 = 5\pi/12$, $\theta_2 = \pi/10\,000$ and $\dot{z}_1 = 1$. It corresponds to the sections in Figure 7.

0.01 leads to a remarkable change: the points are now distributed over two "bands", as shown in Figure 6a. To demonstrate that the points indeed lie on a surface, several slices were made, three of which are shown in Figs. 6b to 6d. These bands begin to dissolve after further increasing L_x up to 0.02 (Figure 7a). The slices in Figs. 7b to 7d clearly show that the points are no longer restricted to a surface, eventhough they remain close to unity.

The spectra reflect this behavior: Fig. 8a ($L_x = 0.01$) displays a clear peak-structure whereas Fig. 8b ($L_x = 0.02$) is already dominated by noise, although there are a number of frequencies whose amplitudes are well above the noise level, which indicates that the motion is not globally chaotic, which would imply the filling of the entire available phase space.

The transition to global chaos ("breaking free") will most likely occur at a later time, owing to Arnold-diffusion. The fact that it does not occur up to $\tau = 50\,000$ indicates that the diffusion can be very slow. If L_x is increased further to $L_x = 0.05$, we finally obtain (observable) global chaos.

A more general study, where, for several values of α, L_x was varied between 0 and the maximum value $L_x^{\max} = \sqrt{3 + 2\alpha - \alpha^2}$ compatible with the geometric structure and the fixed value $E = 1$ of the energy, showed that regular trajectories dominate for small and large angular momenta and that the trajectories for values inbetween are predominantly chaotic. The width of this range inbetween becomes smaller as α increases. In our numerical investigations we did not find a single globally chaotic trajectory for α larger than 2.

4. Summary and Conclusions

In this paper we investigated the dynamics of a freely jointed chain with two mobile mass points and three segments in three dimensions. The Hamiltonian system has three degrees of freedom and two global integrals of motion (energy E and angular momentum L_x about the x-axis). The system is nonlinear due to the constraints requiring constant distances between successive points. Thus, we can expect the system to exhibit chaotic behavior. To our knowledge this is the first system with three degrees of freedom, in which chaos has been investigated and the nonlinearity has its origin not in a potential (which is zero in our case) or boundary conditions [5], but in geometrical constraints.

Eventhough a complete analysis of the dynamics of the chain is impossible (owing to the fact that three initial conditions and two relevant parameters allow a great number of combinations), the dynamics may be summarized as follows:

The most interesting effect is that there are hardly any "normal" regular trajectories, i.e. trajectories

where the points in the Poincaré surface of section are spread over a two dimensional manifold. Most of the trajectories are either over-integrable or chaotic. The results in Figs. 6a to 6d, where the intersection points were indeed distributed over a surface, were an exception. An open question is whether this is a feature peculiar to our specific system or whether this is rather a general feature of systems where nonlinearities are introduced by constraints. Therefore, it might be interesting to study other systems to address this question. Furthermore, one could observe that trajectories tend to be regular for small and large values of L_x and α and that they are mainly chaotic for values inbetween. Finally, we would not find any globally chaotic trajectories for $\alpha > 2$. It should be remarked that in this case the maximum interval of integration was $\tau = 30\,000$ and that a transition to global chaos is possible for greater times, eventhough this is unlikely because of the geometric constraints on the chain for large α. In the present investigations we used equal masses for both points. However, in a previous paper we showed that different masses influence the force-length relation of the chain [8, 26]. Thus, we may also expect an influence of a mass distribution on the dynamics of the points.

Compared to a chain of four segments in two dimensions [6], the present system exhibits more regular behavior, i.e. the increase of the number of degrees of freedom does not necessarily imply an increase in the chaotic behavior.

Acknowledgement

The support of this work by the Deutsche Forschungsgemeinschaft within the Sonderforschungsbereich 239 is gratefully acknowledged.

[1] A. J. Lichtenberg and M. A. Lieberman, Regular and Stochastic Motion, Appl. Math. Sci. Vol. 38, Springer-Verlag, Berlin 1983.
[2] G. Iooss, R. H. G. Hellemann, and R. Stora, Chaotic Behaviour of Deterministic Systems, Les Houches 1981, Session XXXVI, North-Holland, Amsterdam 1983.
[3] P. Bergé, Y. Pomeau, and Ch. Vidal, Order within Chaos, John Wiley & Sons, New York 1984.
[4] R. G. Winkler, Phys. Rev. A **45,** 2250 (1992).
[5] N. De Leon and B. J. Bernie, Chem. Phys. Lett. **93,** 162 (1982).
[6] P. Reineker and R. G. Winkler, Phys. Lett. A **141,** 264 (1989).
[7] R. G. Winkler, Ph.D. Thesis, University of Ulm, Ulm 1989.
[8] G. R. Siegert, Diploma Thesis, University of Ulm, Ulm 1989.
[9] W. Kuhn, Kolloid-Z. **68,** 2 (1934).
[10] W. Kuhn and F. Grün, Kolloid-Z. **101,** 248 (1943).
[11] L. R. G. Treloar, Trans. Faraday Soc. **42,** 71 (1946).
[12] M. V. Volkenstein, Configurational Statistics of Polymeric Chains, John Wiley & Sons, New York 1963.
[13] P. J. Flory, Statistical Mechanics of Polymeric Chains, John Wiley & Sons, New York 1969.
[14] L. R. G. Treloar, The Physics of Rubber Elasticity, 3rd ed., Clarendon Press, Oxford 1975.
[15] M. Doi and S. F. Edwards, The Theory of Polymer Dynamics, Clarendon Press, Oxford 1986.
[16] K. F. Freed, Renormalization Group Theory of Macromolecules, John Wiley & Sons, New York 1987.
[17] J. H. Weiner, Statistical Mechanics of Elasticity, John Wiley & Sons, New York 1983.
[18] G. S. Crest and K. Kremer, Phys. Rev. A **33,** 3628 (1986).
[19] J. H. Weiner, Macromolecules **15,** 542 (1982).
[20] S. K. Kumar, M. Vacatello, and D. Y. Yoon, J. Chem. Phys. **89,** 5209 (1988).
[21] R. G. Winkler, P. Reineker, and M. Schreiber, Europhys. Lett. **8,** 493 (1989).
[22] P. Reineker and R. G. Winkler, Progr. Colloid & Polymer Sci. **80,** 101 (1989).
[23] P. Reineker, R. G. Winkler, G. R. Siegert, and G. Glatting, in: Large Scale Molecular Systems: Quantum and Stochastic Aspects (W. Gans, A. Blumen, and A. Amann, eds.), Plenum Press, New York 1991.
[24] N. G. Van Kampen and J. J. Lodder, Amer. J. Phys. **52,** 419 (1984).
[25] M. Hénon, Physica D **5,** 412 (1982).
[26] P. Reineker, G. R. Siegert, and R. G. Winkler, Colloid & Polymer Sci. **269,** 1090 (1991).
[27] C. D. Conte and C. de Boor, Elementary Numerical Analysis, 2nd ed., McGraw-Hill Kogakusha, Tokio 1972.